PACS numbers: 42.55.Rz; 42.55.Xi; 42.60.Lh
DOI: 10.1070/QE2006v036n07ABEH013178

Continuously tunable cw lasing near 2.75 μm in diode-pumped $Er^{3+}:SrF_2$ and $Er^{3+}:CaF_2$ crystals

T.T. Basiev, Yu.V. Orlovskii, M.V. Polyachenkova, P.P. Fedorov,
S.V. Kuznetsov, V.A. Konyushkin, V.V. Osiko, O.K. Alimov, A.Yu. Dergachev

***Abstract*. CW lasing is obtained in $Er^{3+}(5\%):CaF_2$ and $Er^{3+}(5\%):SrF_2$ crystals near 2.75 μm with 0.4 and 2 W of output powers, respectively, upon transverse diode laser pumping into the upper $^4I_{11/2}$ laser level of erbium ions at 980 nm. Continuous tuning of the laser wavelength between 2720 and 2760 nm is realised in the $Er^{3+}:SrF_2$ crystal.**

Keywords: *IR laser, diode laser pumping, $Er^{3+}:CaF_2$ and $Er^{3+}:SrF_2$ lasers.*

1. Introduction

An $Er^{3+}:CaF_2$ crystal is the first laser medium in which, despite the self-terminating nature of the transition, room-temperature lasing has been obtained in the three-micron region upon up-conversion pumping [1, 2]. The $Er^{3+}:CaF_2$ and $Er^{3+}:SrF_2$ crystals proved to be efficient laser media in the 2.8-μm region both upon direct pumping into the upper $^4I_{11/2}$ laser level by a cw Ti:sapphire laser [3] and up-conversion pumping into the lower $^4I_{13/2}$ laser level [4, 5]. The aim of our paper is to study the possibility of using multisite Er^{3+}-doped fluoride crystals CaF_2 and SrF_2 to obtain efficient and continuously tunable lasing in the 2.8-μm region upon cw diode pumping into the upper $^4I_{11/2}$ laser level.

2. Crystals under study

In CaF_2-ErF_3 and SrF_2-ErF_3 systems, as in other systems formed by fluorides of rare-earth and alkaline-earth elements MF_2-RF_3, broad regions of heterovalent solid solutions of the fluorite $M_{1-x}Er_xF_{2+x}$ structure appear. The limiting molar solubility of ErF_3 in CaF_2 and SrF_2 is 40 % and 43 % ($x = 0.40$ and 0.43), respectively. The parts of phase diagrams of these systems are presented in Figs 1a and 2a [6, 7]. Because the measurement accuracy of the solidus curve of a $Sr_{1-x}Er_xF_{2+x}$ solid solution in [7] was insufficient, we refined it by the method of thermal analysis.

One of the main problems in growing solid-solution crystals $M_{1-x}R_xF_{2+x}$ is the formation of a concentration inhomogeneity – the so-called cellular structure. This phenomenon is caused by the loss of the crystallisation-front stability due to the concentration overcooling appearing because the distribution coefficient of components is different from unity. The distribution coefficients k_0 of ErF_3 in

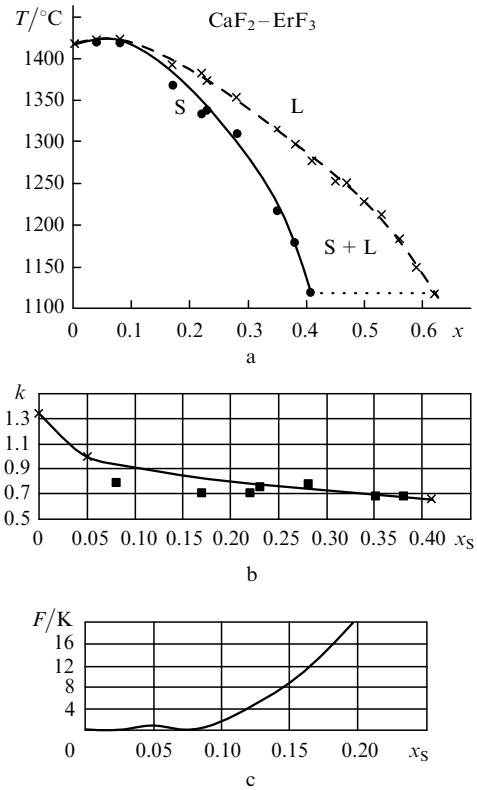

Figure 1. Part of the phase diagram of the CaF_2-ErF_3 system [6]; (×) beginning of solidification [liquidus (L)], (●) beginning of melting [solidus (S)] (a), concentration dependence of the distribution coefficient of ErF_3 upon crystallisation of the solid $Ca_{1-x}Er_xF_{2+x}$ solution from a melt; (×) initial calculation points, (■) experimental data for the phase diagram, the solid curve is the approximation by the expression $k = 1.34 - 0.91x_S^{0.33}$ (b), and the stability of the crystallisation front of solid solutions as a function of the concentration overcooling for the $Ca_{1-x}Er_xF_{2+x}$ system (c).

T.T. Basiev, Yu.V. Orlovskii, M.V. Polyachenkova, P.P. Fedorov, S.V. Kuznetsov, V.A. Konyushkin, V.V. Osiko Laser Materials and Technology Research Center, A.M. Prokhorov General Physics Institute, Russian Academy of Sciences, ul. Vavilova 38, 119991 Moscow, Russia; e-mail: basiev@lst.gpi.ru, orlovski@lst.gpi.ru, marip@lst.gpi.ru, ppf@newmail.ru, tez@rambler.ru, vasil@lst.gpi.ru, osiko@lst.gpi.ru;
O.K. Alimov Institute of Nuclear Physics, Uzbekistan Academy of Sciences, Ulugbek, 702132 Tashkent, Uzbekistan; e-mail: olim@lst.gpi.ru;
A.Yu. Dergachev Q-Peak, Inc., 135 South Road, Bedford, MA, USA

Received 30 March 2006
Kvantovaya Elektronika **36** (7) 591 – 594 (2006)
Translated by M.N. Sapozhnikov

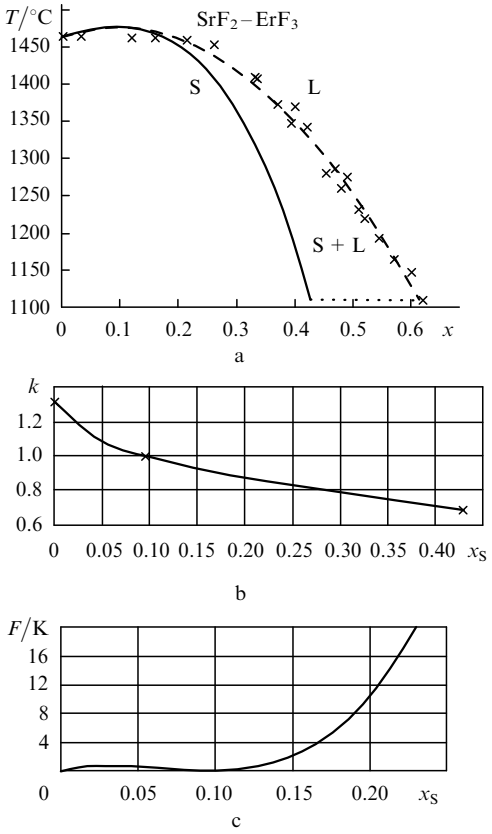

Figure 2. Part of the phase diagram of the SrF_2-ErF_3 system [7]; (×) beginning of solidification [liquidus (L)], (●) beginning of melting [solidus (S)] (a), concentration dependence of the distribution coefficient of ErF_3 upon crystallisation of the solid $Sr_{1-x}Er_xF_{2+x}$ solution from a melt; (×) initial calculation points, (■) experimental data for the phase diagram, the solid curve is the approximation by the expression $k = 1.31 - 0.91x_S^{0.46}$ (b), and the stability of the crystallisation front of solid solutions as a function of the concentration overcooling for the $Sr_{1-x}Er_xF_{2+x}$ system (c).

CaF_2 and SrF_2 at low impurity concentrations (extrapolation to the zero concentration) are close and equal to 1.34 and 1.31, respectively (Figs 1b and 2b) (the method of calculations from the liquidus curve is presented in [8]). For the calcium and strontium systems, the distribution coefficient passes through unity for $x = 0.05$ and 0.096, which corresponds to the maxima of the melting curves of solid solutions. The vicinity of the maximum is optimal for growing crystals with a high degree of homogeneity.

The criterion for stability of the crystallisation front to the concentration overcooling (taking into account only mass transfer processes) can be written in the form

$$\frac{GD}{R} > m\Delta x = F(x), \qquad (1)$$

where G is the temperature gradient at the crystallisation front; R is the crystallisation rate; D is the diffusivity of components in the melt; $\Delta x = x_S - x_L$ is the concentration jump of one of the components (in our case, ErF_3) at the crystallisation front; x_S and x_L are concentrations in the crystal and melt, respectively; and m is the slope of the liquidus curve [9]. The right-hand side of inequality (1) is the stability function $F(x)$ of the crystallisation front having the dimensionality of temperature, which can be found from the phase diagram. The stability functions of the systems under study calculated by the method [9, 10] are presented in Figs 1c and 2c.

The physical sense of the stability function is that when the figurative point of the growing process of a crystal with concentration x, specified by parameters G, R, and D, is located above the curve $F(x)$, the process is stable with respect to concentration overcooling. The stability function $F(x)$ is zero at the extrema of melting curves, i.e., the concentration overcooling is excluded in a homogeneous melt. This determines the choice of $Ca_{0.95}Er_{0.05}F_{2.05}$ compositions for growing single crystals from a melt by the Bridgman method. The $Sr_{0.95}Er_{0.05}F_{2.05}$ composition chosen for the strontium system is not optimal because the stability function vanishes for $x = 0.1$ (Fig. 2c).

Single crystals were grown at the LMTRC, General Physics Institute, RAS by the Bridgman method in a vacuum chamber by using graphite multichannel crucibles and graphite resistance heaters. The crystals were grown in the fluorinating atmosphere of gaseous CF_4 at a pressure of $\sim$0.1 atm. The initial high-purity reagents were also preliminary remelted in the CF_4 atmosphere.

The diffusivity D for the SrF_2-ErF_3 system was absent for calculating the stability parameters of strontium fluorides. The concentration series of $Sr_{1-x}Er_xF_{2+x}$ crystals with the ratio $G/R = 1.94 \times 10^5$ K s cm^{-2} was grown in a multichannel crucible under identical conditions. The concentration stability boundary of the crystallisation front lying between 11.3 % and 15.8 % of ErF_3 was determined by the presence of the cellular structure in grown crystals. Based on these values and the calculated stability function, the diffusion coefficient of cations in the melt was estimated as 4.2×10^{-6} cm^2 s^{-1} $< D < 6.2 \times 10^{-6}$ cm^2 s^{-1}. This value is in good agreement with the data obtained for other SrF_2-RF_3 systems. By using this value, we selected the growth rate of $Sr_{0.95}Er_{0.05}F_{2.05}$ single crystals providing a high optical quality of the crystals (without a cellular structure). Observations in crossed Nicol prisms showed that thermal stresses in the grown crystals were absent.

3. Results and discussion

Spectral and kinetic studies of the grown crystals were performed at LMTRC, General Physics Institute, RAS. Figure 3 shows the absorption spectra of $Er^{3+}(5\,\%):CaF_2$ and $Er^{3+}(5\,\%):SrF_2$ crystals at the $^4I_{15/2} \rightarrow {}^4I_{11/2}$ tran-

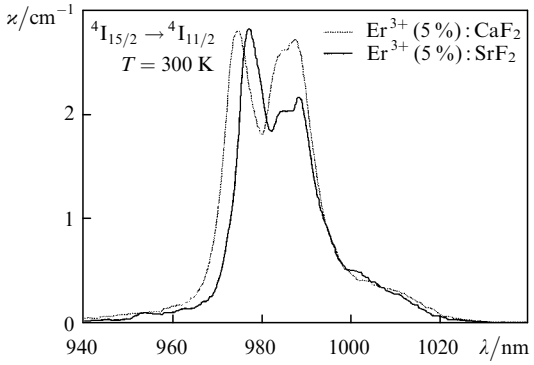

Figure 3. Absorption spectra at the $^4I_{15/2} \rightarrow {}^4I_{11/2}$ transition in the Er^{3+} ion in $Er^{3+}(5\,\%):CaF_2$ and $Er^{3+}(5\,\%):SrF_2$ crystals at 300 K.

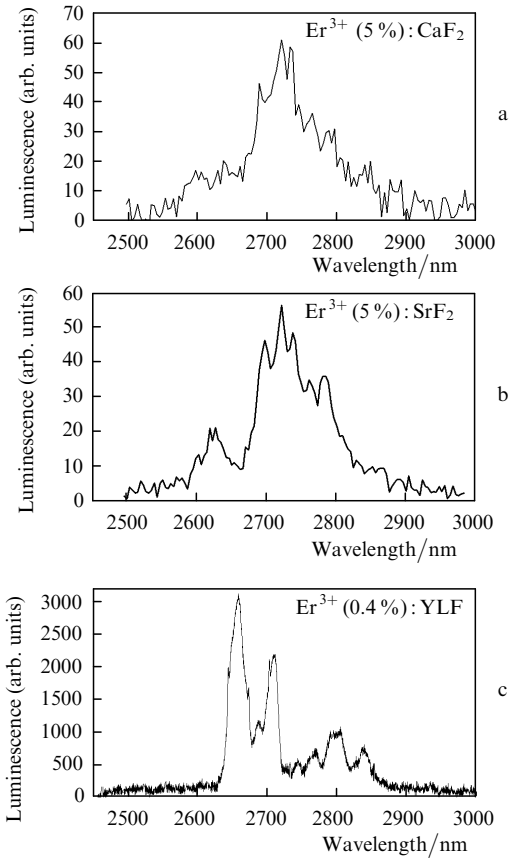

Figure 4. Luminescence spectra at the $^4I_{11/2} \rightarrow {}^4I_{13/2}$ transition in the Er^{3+} ion in $Er^{3+}(5\,\%):CaF_2$ (a), $Er^{3+}(5\,\%):SrF_2$ (b), and $Er^{3+}(0.4\,\%):YLF$ (c) crystals at 300 K excited at 980 nm by a cw diode laser.

sition of the Er^{3+} ion. Absorption coefficients at the 980-nm emission wavelength of diode lasers were $\varkappa = 1.85$ and 2.3 cm^{-1} for the $Er^{3+}(5\%):CaF_2$ and $Er^{3+}(5\%):SrF_2$ crystals, respectively. The luminescence spectra for the $^4I_{11/2} \rightarrow {}^4I_{13/2}$ transition in both crystals were measured at 300 K upon excitation at 980 nm by a cw diode laser (Figs 4a, b). For comparison, Fig. 4c presents the luminescence spectrum of an $Er^{3+}(0.4\,\%):YLF$ crystal. In this crystal doped with 15 % of Er^{3+}, cw lasing was earlier obtained upon direct diode pumping [11].

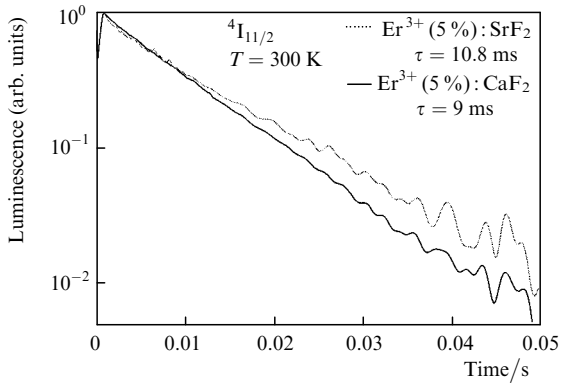

Figure 5. Decay of room-temperature luminescence from the $^4I_{11/2}$ level at 987 nm in $Er^{3+}(5\,\%):SrF_2$ and $Er^{3+}(5\,\%):CaF_2$ crystals excited by a pulsed diode laser at 980 nm.

We measured the luminescence decay at room temperature from the upper $^4I_{11/2}$ laser level at a wavelength of 987 nm for both crystals excited by a tunable pulsed $F_2^+:LiF$ colour centre laser at 980 nm. The luminescence decay of an optically thin $Er^{3+}(5\,\%):SrF_2$ crystal sample in the absence of reabsorption is described by an exponential with the lifetime $\tau = 10.8$ ms, which is somewhat lower than the lifetime $\tau = 12$ ms obtained in [4]. A decrease in the lifetime suggests that both crystals can contain uncontrollable impurities at which luminescence is weakly quenched due to migration of optical excitation energy to these impurities via the $^4I_{11/2}$ level of the Er^{3+} ion.

Laser action in fluoride laser elements was studied by researchers at Q-peak, Inc. (USA) following the experimental method described in [11]. The $Er^{3+}(5\,\%):CaF_2$ and $Er^{3+}(5\,\%):SrF_2$ crystals with Brewster-cut end faces were studied as an active media. The lengths of the $Er^{3+}:CaF_3$ and $Er^{3+}:SrF_2$ crystals were $\sim$15 and 30 mm, respectively. Depending on the crystal length, transverse pumping was performed at 980 nm by one or two linear diode arrays collimated along the fast axis. The maximum pump power of each array was 40 W. The use of transverse pumping in the case of cw lasing reduces stresses in the laser crystal due to a more homogeneous distribution of thermal load over a greater volume compared to longitudinal pumping. We used a thin slab laser element providing reduction of the temperature gradient and stresses in the crystal. The widths of the $Er^{3+}:CaF_2$ and $Er^{3+}:SrF_2$ crystals were 4.9 and 4 mm, respectively. The thickness of both crystals was 1.5 mm. Pumping was performed through polished $1.5 \times (15)$ 30-mm sides, while lasing occurred along the long [15(30) mm] crystal axis, and cooling was performed from two sides through wide unpolished bases of size $4 \times (15)$ 30 mm. Crystals were glued between two water-cooled copper plates.

We used in our experiments a compact symmetric, nearly confocal resonator with two concave mirror of radius 10 cm spaced by $\sim$13 cm. The reflection coefficient of the output mirror was 99 % at a wavelength of 2.8 μm. Figure 6 shows the scheme of the laser setup. All experiments on lasing and wavelength tuning were performed under normal laboratory conditions without purging the resonator with inert gas. CW lasing was obtained at 2.747 nm in a $Er^{3+}(5\,\%):CaF_2$ crystal without a tuning element. The dependence of the output power on the pump power was linear (Fig. 7), with a threshold power of 5 W. The lasing efficiency with respect to the absorbed power was 4 % and the slope efficiency was 4.7 %. The maximum output power for a 15-mm long crystal pumped by one diode array was $\sim$400 mW. We have failed to obtain wavelength tuning in the crystal because lasing disappeared when a tuning element was inserted in the resonator. The increase in the pump power up to 15 W resulted in the thermal damage of the laser crystal. Almost vertical cracks appeared in the crystal (from base to base), their size being considerably greater than the pump beam width of 0.5–0.7 mm. Thus, the volume damage threshold for the $Er^{3+}(5\,\%):CaF_2$ crystal was approximately 500 W cm^{-3}.

The output power obtained for a 30-mm long $Er^{3+}(5\,\%):SrF_2$ crystal pumped by 30-W radiation from two linear diode arrays in the absence of a tuning element was $\sim$2 W. The laser efficiency with respect to the absorbed power was 11 %. The near-field cross section of the Er-laser beam was 3.5×0.6 mm. The beam had the diffraction-

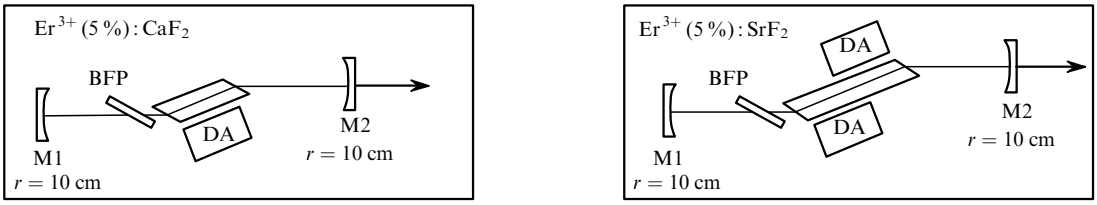

Figure 6. Schemes of continuously tunable cw lasing in $Er^{3+}(5\,\%):CaF_2$ (a) and $Er^{3+}(5\,\%):SrF$ (b) crystals upon transverse diode pumping (M1 and M2: mirrors; DA: linear diode array, BFP: birefringent plate).

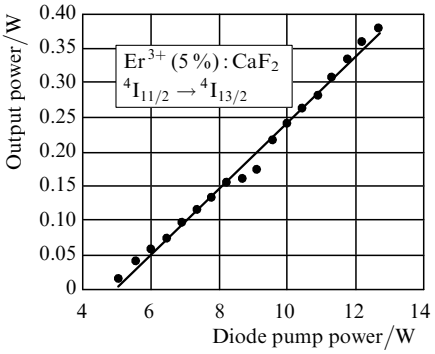

Figure 7. Dependence of the cw output power at 2.8 μm on the 980-nm diode pump power for the $Er^{3+}(5\,\%):CaF_2$ crystal (circles); the solid straight line is the approximation by the expression $y = 0.0479x - 0.238$; the slope efficiency is 4.7 %, the lasing efficiency with respect to the absorbed power is 4 %.

limited divergence in the vertical plane (perpendicular to the plane of Fig. 6). The divergence in the horizontal plane exceeded the diffraction-limited value approximately by 30–40 times.

Laser tuning was performed with the help of a birefringent quartz plate mounted at the Brewster angle. The tuning range of the laser was between 2720 and 2760 nm, the maximum output power being achieved at 2750 nm. In this case, the total pump power provided by two diode arrays was 15 W and the output power at the maximum of the tuning curve was 150–200 mW. The lasing efficiency with respect to the absorbed power was 2.2 %. As the total pump power was increased up to 30 W, cracks appeared in the crystal. Thus, the volume damage threshold for the $Er^{3+}(5\,\%):SrF_2$ crystal proved to be approximately the same as for the $Er^{3+}(5\,\%):CaF_2$ crystal (500 W cm^{-3}).

Tuning of a cw Er laser with the help of a birefringent element was earlier described for a $Er^{3+}(15\,\%):YLF$ crystal in [11]; however, this tuning was performed only discretely over 11 lines. To our knowledge, we have obtained for the first time the continuous tuning of a diode-pumped cw $Er^{3+}:SrF_2$ laser. In the future we expect to obtain a higher output power and intend to study the possibility of broadening the tuning range.

4. Conclusions

Thus, we have obtained cw lasing in $Er^{3+}(5\,\%):CaF_2$ and $Er^{3+}(5\,\%):SrF_2$ lasers at 2.75 μm with 0.4 and 2 W of output powers, respectively, upon transverse diode pumping into the upper $^4I_{11/2}$ laser level at 980 nm. The lasing efficiency with respect to the absorbed power was 4% and 11 %. In the $Er^{3+}(5\,\%):SrF_2$ crystal, continuous tuning between 2720 and 2760 nm has been obtained with a maximum at 2750 nm and the output power ~200 mW. The real lasing efficiency with respect to the absorbed power was 2.2 %. The bulk thermal damage thresholds measured for the $Er^{3+}(5\,\%):CaF_2$ and $Er^{3+}(5\,\%):SrF_2$ crystals proved to be approximately the same and equal to 500 W cm^{-3}.

Acknowledgements. This work was partially supported by the CRDF (Grant No. RU-E2-2585-MO-04) and ISTC-EOARD (Grant No. 2022p).

References

1. Batygov S.Kh., Kulevskii L.A., Prokhorov A.M., Osiko V.V., Savel'ev A.D., Smirnov V.V. *Kvantovaya Elektron.*, 1, 2633 (1974) [*Sov. J. Quantum Electron.*, 4, 1469 (1974)].
2. Gomelauri G.V., Kulevskii L.A., Osiko V.V., Savel'ev A.D., Smirnov V.V. *Kvantovaya Elektron.*, 3, 628 (1976) [*Sov. J. Quantum Electron.*, **6**, 341 (1976)].
3. Labbe C., Doulan J.L., Girard S., Moncorge R., Thuau M. *Proc. Int. Conf. Lasers' 98* (McLEAN, VA: STS Press, 1999) p. 217.
4. Pollack S.A., Chang D.B. *J. Appl. Phys.*, **64**, 2885 (1988).
5. Pollack S.A., Chan D.B., Moise N.L. *J. Appl. Phys.*, **60**, 4077 (1986).
6. Sobolev B.P., Fedorov P.P. *J. Less-Common Metals*, **60**, 33 (1978).
7. Sobolev B.P., Seranian K.B. *J. Sol. State Chem.*, 39, 17 (1981).
8. Fedorov P.P., Turkina T.M., Lyamina O.I., Tarasova E.V., Zibrov I.P., Sobolev B.P. *Vysokochist. Veshchestva*, **6,** 67 (1990).
9. Fedorov P.P. *Neorg. Mater.*, **37**, 95 (2001).
10. Basiev T.T., Voronov V.V., Konyushkin V.A., Kuznetsov S.V., Samartsev A.M., Fedorov P.P. *Trudy VI Mezhdunarodnoi konferentsii 'Kristally: rost, svoistva, real'nya struktura, primenenie'* (Proceedings of VI International Conference on Crystals: Growth, Proprties, Real Structure, and Applications) (Aleksandrov: VNIISIMS, 2003) p. 134.
11. Dergachev A., Moulton P.F. *Adv. Solid-State Photonics*, **83**, 3 (2003).